Journal of Membrane Science 652 (2022) 120445

Contents lists available at ScienceDirect

Journal of Membrane Science

journal homepage: www.elsevier.com/locate/memsci

Combining FTIR spectroscopy and pressure-decay techniques to analyze sorption isotherms and sorption kinetics of pure gases and their mixtures in polymers: The case of CO_2 and CH_4 sorption in polydimethylsiloxane

Valerio Loianno [a,*], Giuseppe Mensitieri [a], Antonio Baldanza [a], Giuseppe Scherillo [a], Pellegrino Musto [b]

[a] Dept. of Chemical, Materials and Production Engineering, University of Naples, Federico II, Piazzale Tecchio 80, Naples, 80125, Italy
[b] Institute for Polymers, Composites and Biomaterials, National Research Council of Italy, Pozzuoli, 80078, Italy

ARTICLE INFO

Keywords:
Gas mixture separation
FTIR Spectroscopy
Transport properties

ABSTRACT

A hyphenated technique combining FTIR Spectroscopy and Barometry is implemented to study transport properties of pure and mixed gases in rubbery polymers. FTIR spectroscopy is operated *in situ* and in the transmission mode. The specific case of transport of pure CO_2 and CH_4 in polydimethylsiloxane (PDMS) was addressed by performing the experimental investigation at ambient temperature and pressure values up to 9 bar, analyzing quantitatively both the gas phase and the solid polymer phase. The IR signals of each species in the gaseous phase were first calibrated against density data of each pure gas. Then, sorption experiments from a unary gas phase were conducted increasing the pressure stepwise and the amount of gas sorbed at each pressure within the polymer was quantitatively determined by measuring the absorbance decay within the gas phase. From these measurements, equilibrium sorption isotherms and sorption kinetics of both pure gases in PDMS have been evaluated. At the same time, FTIR spectra of pure CO_2 absorbed within the polymer phase were collected and calibrated. The spectroscopic contrast in the gas and the polymer phase allowed us to apply the same approaches to sorption of gas mixtures, a very difficult task with the techniques currently available. Preliminary results for the sorption of carbon dioxide from CO_2/CH_4 gas mixtures are presented.

1. Introduction

Polymeric membranes are considered a valid alternative to thermal based separation processes for gas mixtures and liquid chemicals [1–3]. Purification of hydrogen and natural gas from carbon dioxide and other contaminants is a fundamental step for the production of green fuels in a climate-neutral economy [4,5]. Recently, the demand of natural gas increased to replace coal and to face the lack of technologies capable of exploiting renewable energy sources [6]. To understand the separation performances of a polymeric material, sorption and permeation experiments must be conducted in the presence of gas mixtures and new analytical techniques are needed to accomplish this goal more efficiently and rapidly.

Barometry and gravimetry are mostly employed to study transport of pure gases or vapors in polymer films [7]. Usually to retrieve a sorption isotherm curve, stepwise experiments are conducted whereby the pressure and the chemical potential of the unary gas are changed instantaneously. In the case of barometry, the concentration of the penetrant absorbed in the polymer film is indirectly retrieved from a mole balance over the gas phase. Swelling of the polymeric material induced by highly soluble penetrants may change the void volume in the chamber and adversely affect the concentration measurement. Also, when investigating sorption of vapors, their adsorption on the cell surface should be quantified before performing the sorption experiments. Gravimetry is used to infer the penetrant concentration in the polymer from the sample mass variation during sorption [8]. The thermodynamic conditions are kept constant during the experiment and a *zero error* must be corrected due to the buoyancy affecting the sample and the balance components [9]. To conduct sorption measurements of a gas mixture in a polymer, different approaches need to be used. Hopfenberg et al. first coupled gas chromatography with barometry to discriminate the chemical species in the gas phase thereby measuring the gas composition at sorption equilibrium [10]. The mole fraction uncertainty is reported to be generally equal to ±0.01 [11]. Nowadays, this approach is

* Corresponding author.
E-mail address: valerio.loianno@unina.it (V. Loianno).

https://doi.org/10.1016/j.memsci.2022.120445
Received 6 December 2021; Received in revised form 24 February 2022; Accepted 8 March 2022
Available online 17 March 2022

used as a standard both for sorption and mass transport experiments [12, 13]. Fraga et al. recently presented a novel time-lag method to measure the gas components permeabilities with mass spectrometry [14].

In 1974, Lavrent'ev et al. used for the first time FTIR Spectroscopy in the Attenuated Total Reflection (ATR) mode to study the diffusion of liquid acetone in polyisobutylene [15]. Later, in 1992, Shlotter and Furlan studied the diffusion of liquid *n*-decyl alcohol (NDA) in a series of hydrogenated polybutadiene films [16]. They measured the IR spectrum of the penetrant absorbed in the polymer and investigated the NDA signal at 1056 cm^{-1} to retrieve the mutual diffusion coefficient from the IR sorption kinetics. Hong, Barbari and Sloan extended this approach to polymers in contact with vapors. Specifically, they investigated *in situ* sorption of pure Methyl Ethyl Ketone (MEK) vapor in Polyisobutylene (PIB) and separately used gravimetry to calibrate the absorptivity of the MEK IR signal of interest in the polymer phase [17]. This work was propaedeutic to the multicomponent diffusion study of MEK and Toluene vapor mixtures in PIB they subsequently conducted [18]. The authors mainly focused on the measurement of the diffusivities of the two components absorbed in the polymer but also quantified their concentrations in the ternary polymer mixture thanks to the absorptivity of the IR signals of MEK and toluene absorbed in the polymer which had been previously calibrated with pure gas sorption experiments. Afterwards, Kazarian and co-workers used FTIR-ATR Spectroscopy to study sorption of pure supercritical fluids and, specifically, carbon dioxide in polymer films [19]. Only recently, Beckingham et al. used FTIR-ATR Spectroscopy to measure the permeability of liquid methanol, sodium formate, and sodium acetate mixtures through a Nafion® 117 membrane [20]. The mentioned approaches return macroscopic mass transport properties of the polymer – penetrant systems and a more detailed chronological history of the advancement in this field may be found in the literature [21]. Among other applications of IR Spectroscopy to the field of mass transport properties of low MW molecules in solid materials, it is worth mentioning the contributions of J. Kärger and co-workers who applied microimaging techniques based on Interference and Infrared Microscopy (IFM and IRM) to the measurement of the spatially and temporally resolved profile of pure and mixed vapor or gaseous penetrants adsorbed in nanoporous materials (zeolites) [22–24].

Our research group designed and performed sorption experiments based on the synergy between gravimetry or barometry and FTIR Spectroscopy applied *in situ* in the transmission mode. The transport properties of low MW compounds in epoxy resin, polyimides and polybenzimidazole were quantified and qualitative information on the microscale host-guest interactions were retrieved [25–28]. Recently, we proposed a hyphenated approach coupling barometry and FT-NIR Spectroscopy [29]. This approach allows to measure concurrently the solubility of the penetrant within the polymer, the transport properties of the polymer – penetrant system, the polymer swelling induced by the penetrant and the host-guest interactions. In all the previous investigations, we have always studied systems consisting in a polymer in contact with a unary gas phase.

In this work, the gas phase surrounding the polymer sample was analyzed using FTIR Spectroscopy in the transmission mode to quantify the penetrant solubility into the polymer. Sorption of CO_2 and CH_4 in polydimethylsiloxane at ambient temperature and up to 9 bar was chosen as a case study. To this aim, the gas IR spectrum was first calibrated against independent barometric measurements and density data taken from the literature [30]. Measurement errors and properties are discussed. Second, sorption experiments were conducted stepwise both in the case of polymer sample placed within the optical path of the IR beam and in the case in which the sample is located outside of it. In the former case, the IR signals of carbon dioxide in the polymer phase were collected as well. Last, both spectroscopic approaches related to the gas and the condensed phases were exploited to investigate sorption of gas mixtures. This study aims to define a systematic and comprehensive method based on FTIR Spectroscopy in the transmission mode to study gas separation in the membrane technology field.

2. Theoretical background

2.1. FTIR spectroscopy: quantitative analysis

When a chemical species interacts with an electromagnetic radiation, it absorbs part of its intensity. The Lambert and Beer law states that the absorbance intensity at a specific radiation frequency f depends on the molar concentration C of the absorbing chemical species as follows:

$$A(f) = \varepsilon(P, T, f) \cdot L \cdot C \tag{1}$$

where A is the absorbance peak intensity (or *peak height*) of species i, L is the optical path length and ε is the molar absorptivity of the analyzed absorbance peak. The molar absorptivity depends both on the radiation frequency and on the pressure and temperature of the analyzed system. Usually, Eq. (1) has the form of a linear relation between the absorbance signal intensity and the chemical species concentration. At a specific radiation frequency, sources of deviation from linearity are essentially due to the pressure and temperature dependence of the absorptivity, the chosen baseline correction and the detector response. The baseline correction is needed to correct scattering phenomena occurring when the light beam interacts with the sample.

The Lambert-Beer law also applies to the definite integral of a specific IR band (or *peak area*) over the frequency range $[\nu_1, \nu_2]$ as follows:

$$\mathscr{A} = \int_{\nu_1}^{\nu_2} A(f)df = \int_{\nu_1}^{\nu_2} \varepsilon(P, T, f)df \cdot L \cdot C = \overline{\varepsilon} \cdot L \cdot C \tag{2}$$

If the dependence of the molar absorptivity on the temperature and the pressure is negligible, then $\overline{\varepsilon}$ (integrated molar absorptivity) may be assumed constant as well and a modified Lambert-Beer law is applicable. Eq. (2) is preferred whenever an isolated well resolved peak cannot be identified and studied through Eq. (1). Worth noting, Eqs. (1) and (2) are valid whenever a unique chemical component is absorbing IR light in the frequency range investigated (*univariate analysis*). When multiple species are absorbing IR radiation at a specific frequency f and they are not physically or chemically interacting with each other, the resulting IR absorbance signal is equal to the sum of each component. In this case, a *multivariate analysis* should be performed to resolve each contribution. *Difference Spectroscopy* is applied when simple additivity of these contributions is confirmed.

A concentration calibration curve is simply obtained by inversion of Eqs. (1) and (2). Its static sensitivities, respectively $\mathscr{S}$ and $\overline{\mathscr{S}}$, are retrieved as follows:

$$\mathscr{S} = \frac{1}{\varepsilon \cdot L} \; or \; \overline{\mathscr{S}} = \frac{1}{\overline{\varepsilon} \cdot L} \tag{3}$$

Alternatively, by normalizing the absorbance or the integrated absorbance over the optical path length L, the static sensitivity becomes equal to the reciprocal of the molar absorptivity or the integrated molar absorptivity. When non-linearities are observed the sensitivity is calculated from the first derivative of the calibration curve and it will depend on the analyte concentration. The IR absorbance resolution is generally estimated to be equal to three times the noise level affecting it. This is the minimum intensity of the IR signal that could be detected over the random noise largely due to the detector response and it is called limit of detection (LOD). To enhance the signal to noise ratio, multiple scans are usually performed and the mean average spectrum calculated.

2.2. Thickness measurement with FTIR spectroscopy in the transmission mode

FTIR Spectroscopy allows to measure the thickness of a polymer film.

Specifically, it is useful when the thickness is lower than 5 μm and a standard mechanical micrometer cannot be used. By comparison of the FTIR spectra of the specimen under investigation and of a reference sample whose thickness is known, the Lambert-Beer law allows to estimate the unknown thickness as follows:

$$\begin{cases} A_s^{ref} = \varepsilon \cdot L_{s,ref}^0 \cdot C_s \\ A_s = \varepsilon \cdot L_s^0 \cdot C_s \end{cases} \tag{4}$$

where ε is the molar absorptivity of an isolated and well resolved absorbance peak, which is characteristic of the polymer and is measured under high vacuum (dried polymer), A_s^{ref} and $L_{s,\,ref}^0$ are, respectively, the absorbance value and thickness of the reference sample while A_s and L_s^0 refer to the investigated specimen and C_s is the polymer density expressed in terms of molar concentration of repeating units absorbing IR light at the investigated frequency. Then, the unknown thickness value L_s^0 is evaluated as:

$$L_s^0 = \frac{A_s}{A_s^{ref}} \cdot L_{s,ref}^0 \tag{5}$$

FTIR Spectroscopy also allows to measure the polymer thickness variation due to sorption induced swelling. Flichy et al. first applied FTIR-ATR Spectroscopy to monitor this phenomenon when supercritical carbon dioxide is absorbed in a polydimethylsiloxane membrane [31]. Giacinti Baschetti et al. extended this approach to vapors sorbed in glassy polymer films [32]. In a previous contribution we demonstrated that, by using FTIR Spectroscopy in the transmission mode, one can directly relate the intensity decrease of the IR signals of the polymer to the sorption induced swelling $\left(\frac{\Delta V}{V_s^0}\right)$ as follows [29]:

$$\frac{\Delta V}{V_s^0} \cong \frac{3}{2}\left(\frac{A_s^0}{A_s^{eq}} - 1\right) \tag{6}$$

under the assumptions that dilation is isotropic, the small displacements theory is applicable to the system under investigation, the polymer absorbance signal is well resolved, isolated and not affected by specific interactions occurring between the matrix and the absorbed gas (also called in the following penetrant or probe). In Eq. (6), V_s^0 is the specimen volume under high vacuum, ΔV the specimen volume variation due to sorption of the species from the gas phase, A_s^0 and A_s^{eq} the polymer absorbance signal at high vacuum and at equilibrium with the gas phase at specific thermodynamic conditions. The assumed hypotheses also imply that:

$$\frac{\Delta V}{V_s^0} \cong \frac{3\Delta L_s}{L_s^0} = \frac{3\left(L_s - L_s^0\right)}{L_s^0} \tag{7}$$

from which

$$L_s \cong \frac{L_S^0}{2} \cdot \left(\frac{A_S^0}{A_S^{eq}} + 1\right) \tag{8}$$

L_s is the correct thickness value of the specimen at equilibrium with a gas phase at specific thermodynamic conditions. Loianno et al. [29] also showed that a broad band consisting of multiple signals may be analyzed instead of an isolated peak provided the above hypotheses hold true.

Alternatively, if the optical path length were known, the polymer thickness under high vacuum and its variation could be measured from the gas phase spectrum analysis. The gas phase absorbance spectrum is measured with ($A_s^{gas}(T,P)$) and without the polymer sample ($A_{bkg}^{gas}(T,P)$) in the optical path of the IR beam at the same thermodynamic conditions:

$$\begin{cases} A_{bkg}^{gas}(T,P) = \varepsilon \cdot L \cdot C^{gas}(T,P) \\ A_s^{gas}(T,P) = \varepsilon \cdot (L - L_s) \cdot C^{gas}(T,P) \end{cases} \tag{9}$$

where $C^{gas}(T,P)$ is the density of the gas at the temperature T and pressure P. In the following, the gas IR signal is assumed to be isolated from the polymer spectrum and to be well resolved. If the penetrant absorbance contribution is negligible at the same frequency, then, the specimen thickness is derived as follows:

$$L_s = \left(1 - \frac{A_s^{gas}}{A_{bkg}^{gas}}\right) \cdot L \tag{10}$$

If additional contributions from the penetrant spectrum are present at the investigated frequency, *Difference Spectroscopy* allows to isolate them by removing the gas spectrum contribution as follows:

$$A_s^{gas}(T,P) - k \cdot A_{bkg}^{gas}(T,P) = 0 \tag{11}$$

where the factor k is manually calculated. Eq. (11) may be rewritten as follows:

$$k = \frac{A_s^{gas}}{A_{bkg}^{gas}} \tag{12}$$

and, by combining Eqs. (10) and (12), L_s is equal to:

$$L_s = (1 - k) \cdot L \tag{13}$$

Eq. (13) returns the correct value of L_s due to sorption induced dilation at the imposed thermodynamic conditions. If the thermodynamic conditions at which A_s^{gas} and A_{bkg}^{gas} were measured are different, an additional factor takes into account the gas phase density ratio.

3. Experimental

3.1. Materials

Polydimethylsiloxane films were prepared from PDMS Sylgard 184 (Dow Chemicals, Milan, Italy) including a base elastomer and curing agent with a weight ratio of 10:1. These two components were mixed and the solution degassed in a desiccator for half an hour. The solution was then poured upon a PMMA sheet prepared *ad hoc* (Fig. S1 - see *Supplementary Material*) and left at room temperature to be cured overnight. After the curing process, the PDMS substrate is separated from the PMMA structure. The specimen thickness is measured with a Mitutoyo IP65 digital micrometer (uncertainty of ±0.002 mm) and it is equal to 1.295 ± 0.006 mm. Its density is measured by flotation in a water – $CaCl_2$ solution and is equal to 1.034 g cm^{-3}. Pure carbon dioxide with molar fraction purity 999950 μmol mol^{-1} was supplied by Sol S.p.A. (Monza, Italy) and pure methane with molar fraction purity 999995 μmol mol^{-1} was supplied by Nippon Gases Industrial Sud S.r.l. (Naples, Italy). A pure water density standard (CAS number 7732-18-5) and anhydrous $CaCl_2$ (CAS number 10043-52-4) in the powder form with 99.99% purity were purchased from Sigma-Aldrich (Milan, Italy).

3.2. Methods

A schematic diagram of the apparatus is presented in Fig. 1. Specifically, two mass flow controllers type GM50A-013102RMM020 from MKS Instruments (Full scale volumetric flow range of N_2 100 sccm) were added to the system proposed by Loianno et al. [29] upstream of the charge chamber (in the following, chamber 1). The uncertainty is ±1% of setpoint for flow rates greater than 20% full scale flow range and 0.2% full scale flow range for flow rates greater than 2% and smaller than 20% full scale flow range. The resolution is equal to 0.1 sccm. The repeatability is ±0.3% of reading and the typical settling time is about 500 ms above 5% full scale flow range. The maximum inlet operating pressure is approximately equal to 11.34 bar. A Baratron 121A pressure sensor from MKS Instruments (Full Scale Pressure Range of 30 bar, accuracy of 0.5% of reading, resolution of 0.003 bar) is connected to chamber 1. The sensor was calibrated by MKS Instruments with the MKS transfer

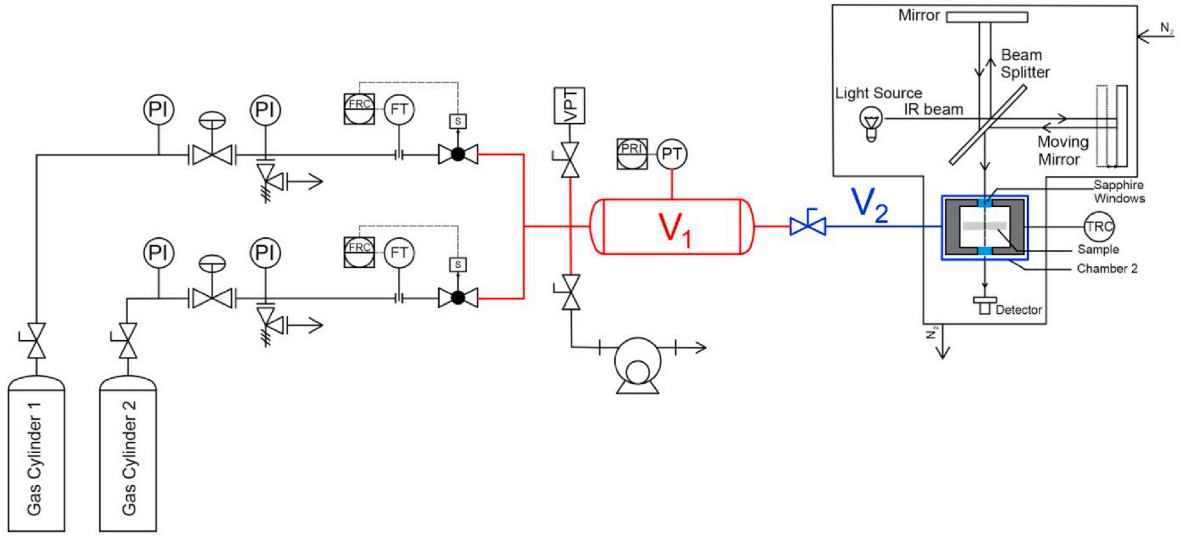

Fig. 1. Schematic diagram of the apparatus. PI: analog pressure indicator; PT: pressure transducer; FT: flow rate transducer; FRC: MKS PR4000B datalogger and controller; PRI: MKS PR4000S datalogger; VPT: vacuum pressure transducer.

standard S/N 78177–6. The latter was calibrated with a CEC Air Dead-weight tester traceable to the National Institute of Standards and Technology (NIST). Gas mixtures are prepared with the mass flow controllers. Volume V_1 is equal to 133.55 cm^3, volume V_2 is equal to 64.11 cm^3 and the total volume of the stainless steel spheres placed in chamber 1 is equal to 40.915 cm^3. The downstream chamber (in the following, chamber 2) works as an IR cell: it is made of stainless steel and it includes two coplanar sapphire windows 1.393 ± 0.001 cm apart from each other. Swagelok VCR fittings are used to make the apparatus leak proof.

A Spectrum 100 spectrometer (Perkin Elmer, Norwalk, CT) measures the FTIR spectra in transmission mode. The interferometer is equipped with a Germanium/KBr beam splitter and the detector is a wide band deuterated triglycine sulfate (DTGS) sensor working at room temperature and having a wavelength response ranging from the near infrared to the far infrared. Chamber 2 windows are made of sapphire and, consequently, the spectral range investigated is limited to 8200–1600 cm^{-1}. The spectrum of the gas phase at equilibrium is collected at 2 cm^{-1} resolution from the mean of 32 co-added scans. The optical path difference velocity is 0.2 cm/s. In these conditions, the time to acquire one spectrum is 9 s. During sorption kinetics, the spectra are recorded continuously at 4 cm^{-1} frequency resolution with the same optical path difference velocity and the acquisition time is 5 s. Onwards, all uncertainties refer to expanded uncertainties at 95% confidence.

4. Results and discussion

4.1. IR gas calibration

The gas IR calibration curves for CO_2 and CH_4 were evaluated from the IR absorbance peak intensity or the area underneath it as a function of the molar concentration of the gas species. The latter is calculated from the NIST Reference Fluid Thermodynamic and Transport Properties Database (REFPROP version 7) knowing the experimental thermodynamic conditions at which the spectroscopic measurement is conducted [30]. Moving from the MIR frequency region (from 200 to 4000 cm^{-1}) to the NIR one (4000–12800 cm^{-1}), the signals corresponding to the fundamental vibrations of each component are mainly replaced by overtone/combination bands (Fig. 2). The black arrows identify the IR peaks of gaseous CO_2 whose calibration curves are presented in Fig. 3. The peak intensity is normalized over the optical path length of the cell.

The fundamental vibration located in the range [2200, 2450] cm^{-1} saturates at 200 mbar approximately, so that it cannot be used for analytical purposes. We considered only the vibrations at 3626, 3729 and 4991 cm^{-1}. The peaks' absorbance calibrations performed at two different temperatures 35 and 26.5 °C, with IR windows made of single crystal Sapphire (thickness 2.25 mm, red data). For comparison purposes, spectra were also collected at 35 °C with IR windows made of ZnSe (thickness 2 mm, blue data). The dependence of the molar absorptivity on the temperature in the range investigated is negligible. The

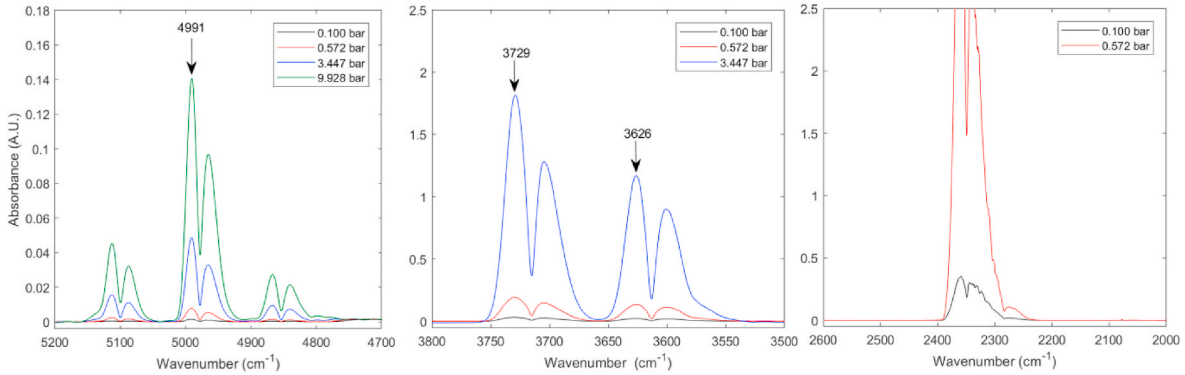

Fig. 2. IR spectra for pure gaseous CO_2 at several pressures obtained with a spectrum resolution of 2 cm^{-1} and sapphire flat coplanar windows at 26.5 °C.

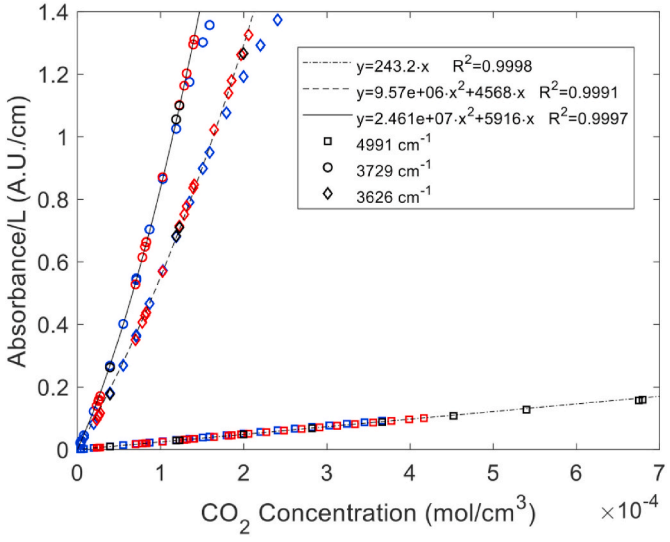

Fig. 3. CO_2 IR calibration curves. Blue data: 35 °C ZnSe windows. Red data: 26.5 °C Sapphire windows. Black data: 35 °C Sapphire windows. Spectrum resolution is 2 cm^{-1}. Baseline correction has been performed in the following frequency ranges: [3400, 3900] cm^{-1} for the signal at 3729 cm^{-1}, [3527, 3657] cm^{-1} for the signal at 3626 cm^{-1} and [4908, 5029] cm^{-1} for the signal at 4991 cm^{-1}. (For interpretation of the references to colour in this figure legend, the reader is referred to the Web version of this article.)

radiation energy reaching the detector is lower in the case of ZnSe (see Fig. S2 in *Supplementary Material*) and, consequently, a deviation from the trend of the calibration curve with sapphire windows is observed at absorbance values higher than 1 A U.·cm^{-1} (see Fig. 2).

The signal at 4991 cm^{-1} shows a good linear dependence on the concentration, so that the experimental data were fitted with a linear expression. The molar absorptivity associated to this signal, as retrieved from the linear least-square regression analysis of the data, is equal to 243.2 ± 0.7 cm^2 mol^{-1} with a R-square of 0.9998 and a root mean squared error (or RMSE) of 4.064•10^{-4} A U.·cm^{-1}. The other two signals analyzed in Fig. 2 show a slightly non-linear parabolic behavior, likely due to a pressure broadening effect and to the detector response. A second order polynomial of the form $a_1 \cdot x^2 + a_2 \cdot x + a_0$ (where the coefficient a_0 is set to zero) was fitted to each set of data and the results are reported in Table S1 (see *Supplementary Material*).

In Fig. 4, three regions of the IR spectrum of pure gaseous CH_4 are reported as a function of pressure at 27 °C. The fundamental vibration centered at 3000 cm^{-1} saturates at 0.5 bar approximately and has not been considered for analytical purposes, but the two wings corresponding to the P and R branches of the vibrational-rotational spectrum only saturates at 3.5 bar approximately. The black arrows identify the peaks that have been used for quantitative evaluations. The associated IR calibration curves are reported in Fig. 5 and show a negligible dependence on the temperature in the 27–35 °C range. The whole set of calibration curves was best fitted with a second order polynomial function whose intercept was imposed to be zero. Again, the observed deviation from linearity is associated with a pressure broadening effect and with the detector response. The same procedure used here to obtain the IR calibration curves could be used for any heteronuclear gas species.

A continuous gas IR calibration curve has been also obtained by using the automated solenoid valve of the thermal mass flow controller to slowly but steadily increase the pressure of the pure gas inside the IR cell. The flow rate was set equal to 15 sccm and the software Timebase® from Perkin Elmer was used to record continuously the IR spectrum at 4 cm^{-1}. The pressure and the IR spectrum were measured simultaneously and, following the approach adopted in Figs. 3 and 5, the gas IR peaks

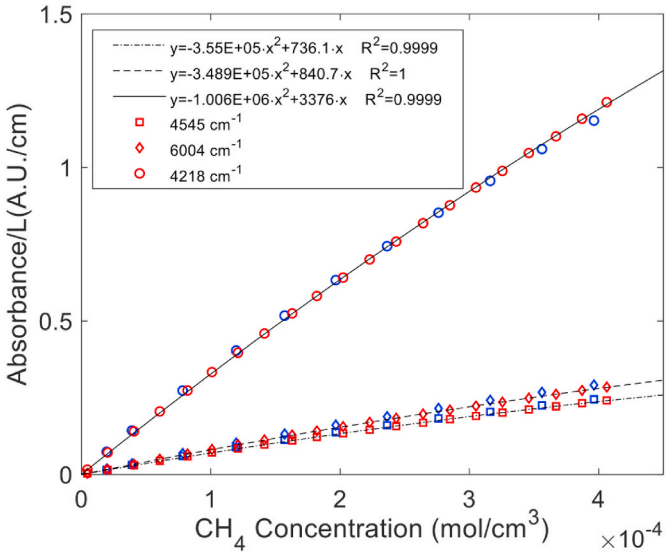

Fig. 5. CH_4 IR calibration curves. Blue data: 35 °C ZnSe windows. Red data: 27 °C Sapphire windows. Spectrum resolution is 2 cm^{-1}. Baseline correction has been performed in the following frequency ranges: [3565, 4821] cm^{-1} for the signal at 4218 cm^{-1}, [5300, 6500] cm^{-1} for the signal at 6004 cm^{-1} and [4526, 4564] cm^{-1} for the signal at 4545 cm^{-1}. (For interpretation of the references to colour in this figure legend, the reader is referred to the Web version of this article.)

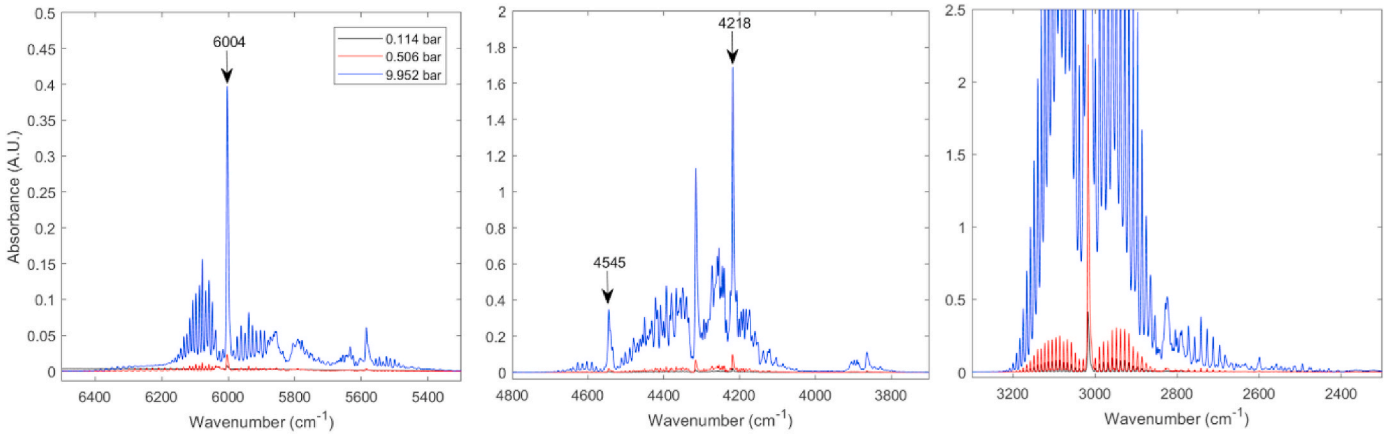

Fig. 4. CH_4 IR spectra obtained with a spectrum resolution of 2 cm^{-1} and sapphire flat coplanar windows at 27 °C.

were correlated with the gas density (see Fig. S3 in *Supplementary Material*). An excellent agreement was obtained between the dynamic and the static calibration curves thus confirming that, at any time during the dynamic calibration, the system can be considered as being at thermodynamic equilibrium. The uncertainty of the absorbance and the gas concentration values in Figs. 3 and 5 is within the size of reported symbols.

Once the calibration curves for the IR signals have been obtained, in turn the IR signals can be used during a sorption experiment to retrieve the molar concentration in the gaseous phase, even in the case of gas mixtures. As an example, we present the gas concentration specifications for the calibration of the CO_2 signal at 4991 cm^{-1}. The absorbance resolution is estimated from the LOD. At 4500 cm^{-1}, it is equal to $1 \cdot 10^{-3}$ A U. The resolution of molar concentration is calculated from the ratio of the absorbance resolution and the product of the optical path length with the signal molar absorptivity and it is equal to $3 \cdot 10^{-6}$ mol cm^{-3}. The linear fitting of the data returns a RMSE of $1.671 \cdot 10^{-6}$ mol cm^{-3}. The full-scale output range (FSO) equals $4.16 \cdot 10^{-4}$ mol cm^{-3}. The maximum linearity error is equal to 1% FSO. The full scale input range (FSI) equals 0.1 A U.·cm^{-1}. The static sensitivity is equal to $4.111 \cdot 10^{-3}$ mol cm^{-3} and the sensitivity error is equal to $1.2 \cdot 10^{-5}$ mol cm^{-3}. The concentration uncertainty was estimated from the *root-sum-squares* method (*RSS*) and the uncertainty budget is presented in Table S2. The following sources of error were taken into account: the linearity and the sensitivity of the calibration curve, the pressure transducer, the IR absorbance uncertainty, the error propagation of the pressure over the gas density retrieved from the NIST REFPROP 7 database. The concentration uncertainty estimated from the IR absorbance measurement is then equal to $4.5 \cdot 10^{-6}$ mol cm^{-3}. A second order polynomial of the form $a_1 \cdot x^2 + a_2 \cdot x$ reduces significantly the RMSE value. An analogous procedure could be applied to any other CO_2 signal and in the case of CH_4 as well. Hysteresis effects were never observed.

A key aspect of vibrational spectroscopy is the great number of signals available for the investigation of the gas concentration. Each of them represents an independent and individual measurement. Therefore, to increase the sensitivity of the concentration calibration curve, the outputs (absorbance or integrated absorbance value) of multiple signals may be added to each other at fixed thermodynamic conditions. Overtones and combination bands also allow to tune the FSO and the uncertainty of the gas concentration (more on this later).

4.2. Pressure decay vs absorbance decay: pure CO_2 and CH_4

Stepwise sorption experiments of pure CO_2 and CH_4 in PDMS were conducted up to 9 bar and at ambient temperature. In a typical experiment, chamber 1 is first filled with a specific concentration of one gas which is then expanded into chamber 2. Prior to the gas expansion, the sample chamber may be either under high vacuum (integral step) or at a specific concentration of the gas (differential step). The polymer film was placed in chamber 2 either along the optical path of the IR beam (referred to as 'test β', performed with a sample of mass equal to 2.1813 g) or outside of it (referred to as 'test α', performed with a sample of mass equal to 5.4325 g). Tests β were performed to collect IR signals also from the polymer phase which contains the absorbed gas molecules. The pressure and the IR spectrum in the gas phase were recorded simultaneously during the experiment to monitor the gas concentration decay. Quantification of the sorption thermodynamics and mass transport is accomplished with both methods to highlight the performances of the spectroscopic approach.

4.2.1. Sorption equilibrium

Fig. 6-A compares the CO_2 and CH_4 sorption isotherms in PDMS obtained barometrically at ambient temperature with data taken from the literature [11,29,33]. Other studies have been conducted in the past on the same polymer – pure penetrants system and are consistent with the results presented herein [34–37]. At a specific temperature, the pressure measurement is converted into the molar concentration of the pure gas with the NIST Reference Fluid Thermodynamic and Transport Properties Database (REFPROP version 7) [30]. A mole balance over the gas phase during the sorption experiment returns the concentration of the compound absorbed within the polymer. The photometric signals of CO_2 at 4991 cm^{-1} and of CH_4 at 4218 cm^{-1} were analyzed at thermodynamic equilibrium and the molar concentration in the gas phase was determined on the basis of the II order polynomial fitting for the corresponding concentration calibration curves. In Fig. 6-B, the equilibrium gas concentrations obtained from vibrational spectroscopy are compared with results from barometry. The uncertainty of the gas concentration values in Fig. 6-B is within the size of reported symbols. For tests α, the evaluation of gas concentration is straightforward because no change of the optical path occurs. Conversely, in the experimental configuration of test β, the collected spectrum includes the contributions of the gas phase, of the polymer and of the penetrant absorbed into the polymer. In the frequency region under investigation, the contribution of the gas phase to the total spectrum was isolated by removing the other two contributions using *Difference Spectroscopy*. Evaluation of the correct polymer spectrum (A_s^{eq}) to be subtracted should be performed accounting for sorption induced swelling $\left(\frac{\Delta V}{V_s^0}\right)$ at the operating thermodynamic conditions. This is given by the following expression:

$$A_s^{eq}(T,P) = \left(1 + \frac{2}{3}\cdot\frac{\Delta V}{V_s^0}\right)^{-1} A_S^0 = \overline{k}\cdot A_s^0 \tag{14}$$

where the symbols have been defined in Section 2.2 and $\overline{k}$ is calculated manually. Subtraction of separate and isolated polymer signals may improve the evaluation of $\overline{k}$. It is recalled here that Eq. (14) is derived by assuming isotropic swelling, the validity of the small displacement

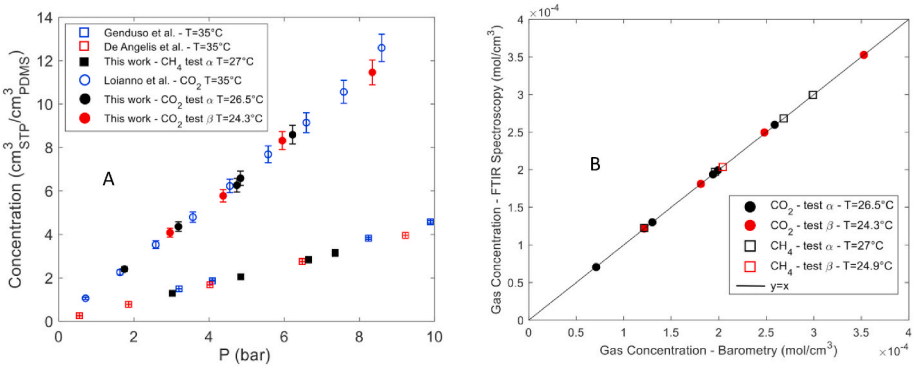

Fig. 6. A: barometric sorption isotherms of CO_2 and CH_4 in PDMS [11,29,33]. B: comparison of the equilibrium gas concentration with the two methods.

theory and the absence of polymer – penetrant interactions.

Difference Spectroscopy is applied once again to isolate the penetrant spectrum from the gas phase spectrum. The subtraction procedure is reported in Section 2.2 where a correction factor k is defined to take into account the optical path length reduction due to the polymer specimen. The experimental gas spectrum A^{gas} is finally retrieved as follows:

$$A^{gas}(T,P) = \frac{L - L_s}{L} \cdot A^{gas}_{bkg}(T,P) = k \cdot A^{gas}_{bkg}(T,P) \tag{15}$$

where the symbols have been defined in Section 2.2. After normalization of A^{gas} over the effective optical path length, the gas concentration is calculated from the concentration calibration curve presented in Figs. 3 and 5.

Examples of the application of this protocol are presented onwards. The sorption test β of carbon dioxide in PDMS at 8.345 bar and 24.3 °C is analyzed using the peak at 4991 cm^{-1}. The polymer contribution is negligible at this specific frequency so that swelling effects may be discarded ($\bar{k} \cong 1$). Subtraction of the dry polymer absorbance spectrum returns the *difference spectrum* in Fig. 7-A. Then, the absorbed CO_2 band centered at 4954 cm^{-1} is isolated by subtracting the background gas spectrum (blue line) corrected with a factor k equal to 0.900. The latter may be evaluated manually or from Eq. (12). being the specimen thickness known. In Fig. 6A, the background gas spectrum is compared with the *difference spectrum*, the correct gas spectrum and the penetrant spectrum. This procedure is applied to every sorption test β of CO_2 in PDMS presented in Fig. 6-A. The difference between the spectroscopic and the barometric gas density is 0.1% of the equilibrium value. The deviation from the correct equilibrium value would increase up to 1% if the subtraction protocol were not used.

The sorption test β of methane in PDMS at 5.036 bar and 24.9 °C is studied using the peak at 4316 cm^{-1}. Methylene and methyl groups' vibrations characterize both PDMS and methane. Therefore, the polymer spectrum is first subtracted with a correction factor $\bar{k}$ equal to 0.997. Subsequently, the absorbed CH_4 spectrum is isolated from the gas phase spectrum by subtraction of the background gas spectrum (blue line) with a correction factor k equal to 0.916. In Fig. 7-B, the comparison between the spectra of the background gas, the gas at the experimental conditions, the penetrant and the *difference spectrum* is presented. The contribution of the absorbed penetrant spectrum and the polymer swelling is negligible over the experimental gas signal.

The subtraction protocol is conducted manually. The task does not require much effort since other signals related to the polymer and the penetrant are available and, being the two correction factors frequency independent, the procedure is applicable to all of them as well. Finding the IR bands where one of the two correction factors equals unity facilitates the evaluation of the remaining one. This is accomplished by looking for a frequency region where one of the three spectral contributions (polymer, gas, penetrant) is absent. Both values of $\bar{k}$ and k return quantitative information about the specimen thickness, i.e. the polymer swelling, at the operating thermodynamic conditions allowing to double check the correctness of the subtraction protocol. This analysis confirms that FTIR Spectroscopy allows an accurate measurement of the gas concentration at thermodynamic equilibrium and also allows to discriminate the chemical species present in the gas phase.

4.2.2. Sorption kinetics

The sorption kinetics of CO_2 and CH_4 in PDMS were obtained spectroscopically and barometrically from the gas concentration decay of tests α and the results are compared here to each other. The spectra were recorded at 4 cm^{-1} frequency resolution so that the acquisition time for a single spectrum measurement was 5 s. This is a good compromise to enhance the signal to noise ratio although each measured absorbance value actually corresponds to the average concentration monitored during the IR spectrum acquisition time. Therefore, the experimental time that was assigned to each absorbance value has been calculated as the nominal time of acquisition reduced by 2.5 s. The diffusion time in the case at hand is on the order of minutes and, consequently, the effect of this correction is relevant only at the initial stage of the sorption kinetics.

Sorption test α of CO_2 in PDMS is here analyzed as an example. The absorbance dynamics of the peak height at 3626 cm^{-1} for three sorption steps (respectively, an integral step up to 4.740 bar, an integral step up to 1.753 bar and a differential step from 1.753 to 3.186 bar) are compared in Fig. 7. Although the gas concentration decrement registered during the integral step up to 4.740 bar (Fig. 7-A) more than doubles each decrement associated to the other two sorption steps presented in Fig. 7-B and 7-C, the absorbance decay is noisier and the uncertainty at equilibrium is equal to $5.05 \cdot 10^{-3}$ A.U. cm^{-1} as compared to the lower values of $3.5 \cdot 10^{-4}$ and $1.3 \cdot 10^{-3}$ A.U. cm^{-1} respectively determined for the integral step up to 1.753 bar and the differential step from 1.753 to 3.186 bar. The relative uncertainty expressed as a percentage of the mean absorbance value at equilibrium is 0.424%, 0.100%, 0.173% respectively.

The sorption kinetics, i.e. the kinetic profile of the probe within the polymer, may be obtained from a mole balance over the gas phase. The number of penetrant moles (n) in the polymer during the diffusion process are equal to:

$$n = n_i^{gas} - n^{gas}(t) \tag{16}$$

where n_i^{gas} is the initial number of moles in the gas phase before the sorption process starts while $n^{gas}(t)$ is the number of moles in the gas phase during the diffusion process. To obtain the sorption kinetics n is normalized over the total amount of moles absorbed equal to

$$n_{tot} = n_i^{gas} - n^{gas}(t \to \infty) \tag{17}$$

By assuming that the polymer dilation is negligible with respect to

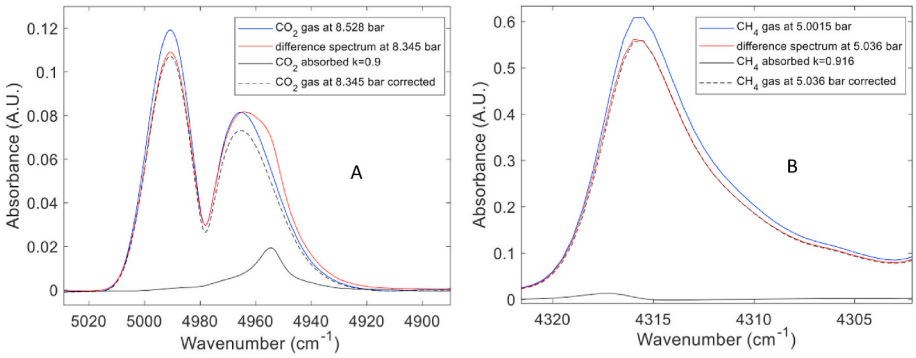

Fig. 7. Sorption of light gases in PDMS during test β. A: CO_2 B: CH_4. Blue trace: gas background spectrum measured in the empty sample chamber. Black solid trace: spectrum of the penetrant. Black dashed trace: gas spectrum at the experimental thermodynamic conditions. (For interpretation of the references to colour in this figure legend, the reader is referred to the Web version of this article.)

the void volume, the following result holds true:

$$n / n_{tot} = C/C_{tot} \tag{18}$$

where C and C_{tot} are the probe mole concentrations in the polymer phase during the diffusion process and at sorption equilibrium respectively. Since a II order polynomial function is chosen to describe the relation between the gas concentration and the peak absorbance, the sorption kinetics is also retrieved as follows:

$$\frac{n}{n_{tot}} = \frac{C}{C_{tot}} = \frac{a\cdot\left(A_i^2 - A(t)^2\right) + b\cdot(A_i - A(t))}{a\cdot\left(A_i^2 - A(\infty)^2\right) + b\cdot(A_i - A(\infty))} \tag{19}$$

where A_i, $A(t)$ and $A(\infty)$ are the absorbance values corresponding to C_i^{gas}, $C^{gas}(t)$ and $C^{gas}(\infty)$ respectively. If the experimental absorbance decay is small compared to the FSI range, the concentration calibration curve is linearized giving the following result:

$$\frac{n}{n_{tot}} \cong \frac{A_i - A(t)}{A_i - A(\infty)} \tag{20}$$

The same line of reasoning is valid for the integrated absorbance $\mathscr{A}$ and the following result is obtained:

$$\frac{n}{n_{tot}} \cong \frac{\mathscr{A}_i - \mathscr{A}(t)}{\mathscr{A}_i - \mathscr{A}(\infty)} \tag{21}$$

The linearization hypothesis is valid for the kinetics shown in Fig. 8. A_i may be calculated from the IR gas calibration curves (see Section 4.1) at $C = C_i$ which is obtained from the barometric measurement and the NIST REFPROP 7 database [30]. Alternatively, A_i is extrapolated from a linear regression of the spectroscopic sorption kinetics at short times. Since the diffusion of carbon dioxide and methane in PDMS is Fickian and the diffusivity is independent of the penetrant concentration within the polymer phase, this approach applies to the system under investigation and is used onwards [34].

From Eq. (20) the absorbance decay shown in Fig. 8-A, associated to the peak at 3626 cm^{-1}, is converted to the corresponding sorption kinetics in Fig. 9-A. For the sake of comparison, the sorption kinetics retrieved from the peak height at 4991 cm^{-1} and the barometric sorption kinetics are reported as well. The sensitivity of this IR signal is one order of magnitude lower than the 3626 cm^{-1} signal (Fig. 3) but its absolute uncertainty is thirty-five times smaller. Consequently, the relative expanded uncertainties are comparable and equal to 0.36% and 0.42% for the 4991 cm^{-1} and 3626 cm^{-1} signals, respectively. The relative expanded uncertainty is reported as a function of the gas peak height values in Fig. S4 (see *Supplementary Material*). It is independent of the frequency and shows a minimum in the range [0.2, 0.6] A.U. cm^{-1}. The signal at 3626 cm^{-1} returns a sorption kinetics as accurate as the barometric one for the integral sorption step up to 1.753 bar (Fig. 9-B). The scattering of the IR absorbance values is related to the intrinsic uncertainty of the IR measurement. Being FTIR Spectroscopy used in the transmission mode, the uncertainty is a function of the pressure at which the measurement is being conducted. The lowest signal to noise ratio is expected in the low and in the high pressure ranges. At low pressure, this occurs because the intensity of the analytical signal (IR absorbance) is low. At high pressure, the increased scattering is related to the approaching saturation of the gas signal. At intermediate pressures, an optimum range, which depends upon the frequency of the signal, is found where the scattering is at a minimum.

This analysis highlights the potentiality of FTIR Spectroscopy to measure independently sorption equilibrium and mass transport of gases and vapors in polymers. Barometry has a higher sensitivity with respect to FTIR Spectroscopy but cannot discriminate the chemical species in the gas phase. As such, it cannot be extended to the investigation of gas mixtures without being coupled with a separate technique.

The definite integral of a specific IR band may be calculated instead of a single peak intensity. From Eq. (2), the integrated absorbance $\mathscr{A} = \bar{\varepsilon}\cdot L\cdot C$ has a greater static sensitivity than the absorbance $A(f)$. The absolute uncertainty of $\mathscr{A}$ with respect to $A(f)$ increases as well but the relative uncertainty decreases. For instance, in Fig. S5 (see *Supplementary Material*), the integral sorption kinetics of CO_2 in PDMS up to 4.740 bar (test α) is retrieved from the integrated absorbance $\mathscr{A}$ evaluated in the range [3527, 3657] cm^{-1}. The static sensitivity increases fifty times approximately. At equilibrium, the absolute uncertainty of the normalized integrated absorbance signal ($\pm 4.716\cdot 10^{-2}$ A.U. cm^{-2}) is one order of magnitude greater than the absolute uncertainty of the peak height signal at 3626 cm^{-1} ($\pm 4.982\cdot 10^{-3}$ A.U. cm^{-1}) approximately. However, the relative uncertainty decreases from 0.419% down to 0.100%. The same comments hold true in the case of methane and some results are reported in Figs. S6 and S7.

The absorbance decay observed during sorption of the pure gas allows to measure the penetrant concentration within the polymer provided A_i and $A(\infty)$ are independently evaluated from barometry. The expanded uncertainty of the penetrant concentration, expressed in standard cubic centimeters of gas over cubic centimeters of dry polymer, is evaluated via the RSS method at 95% confidence. The uncertainty of the following quantities are included: the concentration calibration curve; the void volume; the specimen density; the linear extrapolation of A_i at short times. The concentration calibration curve at 4 cm^{-1} resolution obtained dynamically is used (Fig. S3) and linear interpolation is performed in the concentration region investigated. In Fig. 10, the sorption isotherms of CO_2 in PDMS retrieved from the IR and the barometric analysis are compared to each other. The peak height at 3600 and 3626 cm^{-1} are chosen having a higher sensitivity with respect to the peak at 4991 cm^{-1}. Also, the FSO of the peak at 3600 cm^{-1} spans the whole set of sorption experiments. The signal at 3626 cm^{-1} is chosen for comparison and saturates at 6 bar approximately. The expanded uncertainty of the barometric results is estimated from the error propagation of the following elements: the density value of the NIST

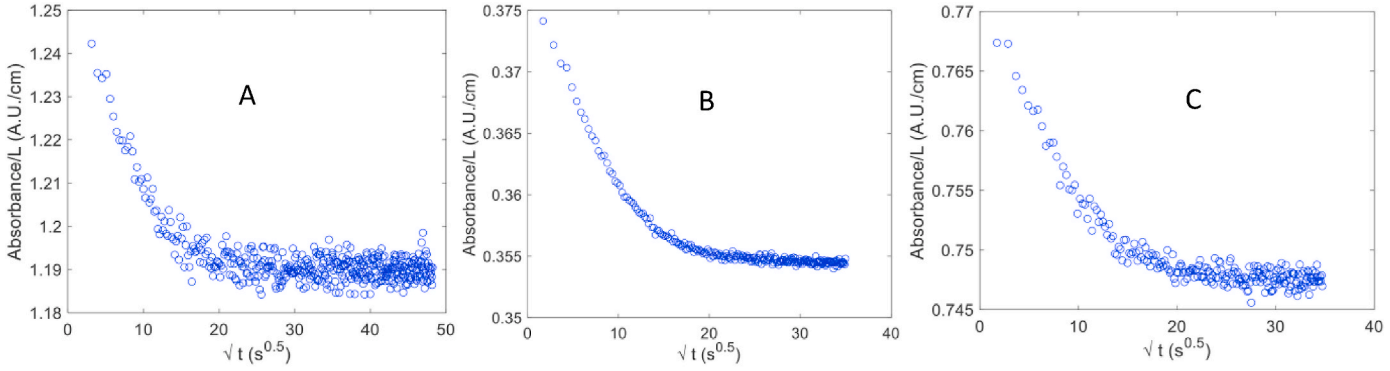

Fig. 8. Sorption of CO_2 in PDMS during tests α tracked with the IR gas phase absorbance decay at 3626 cm^{-1}. A: integral step up to 4.740 bar. B: integral step up to 1.753 bar. C: differential step from 1.753 to 3.186 bar.

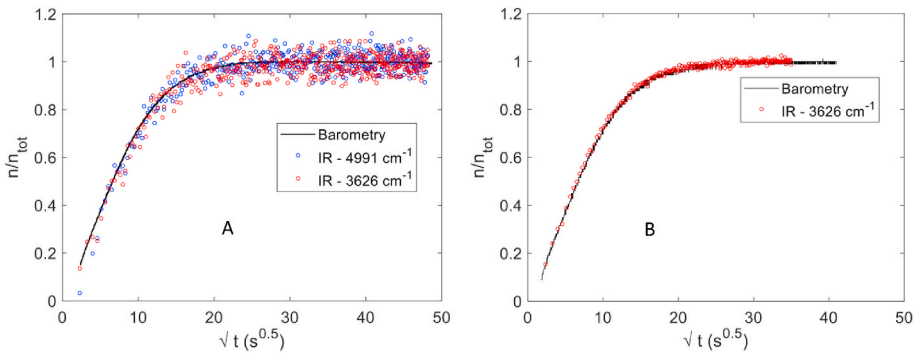

Fig. 9. Sorption kinetics of CO_2 in PDMS (tests α). A: integral sorption step up to 4.740 bar. B: integral sorption step up to 1.753 bar.

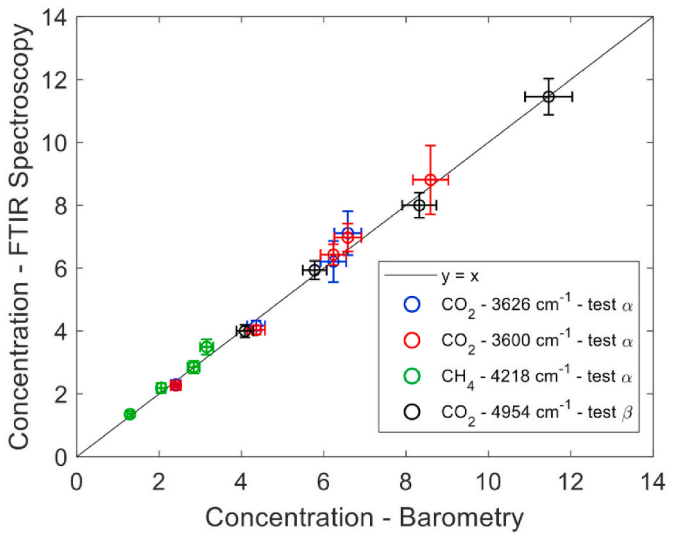

Fig. 10. Concentration of CO_2 and CH_4 in PDMS expressed in $cm^3_{STP} \cdot cm^{-3}_{PDMS}$. Spectroscopic and barometric results are independent from each other.

REFPROP7 database; the specimen volume; the void volume; the uncertainty of the pressure transducer. The sorption isotherm comparison is evaluated for methane as well from the peak at 4218 cm^{-1}.

In the case of test β, the sensitivity and the uncertainty of the gas IR signal at 4991 cm^{-1} does not allow to retrieve an accurate value of A_i. However, in this type of test we can retrieve spectroscopic information directly on the absorbed penetrant. In fact, the IR peak at 4954 cm^{-1} of the spectrum of CO_2 absorbed in PDMS was isolated and used for quantitative evaluations. Its molar absorptivity at 35 °C was retrieved from the literature and it is equal to 0.2992 ± 0.0075 L cm^{-1} mol^{-1} [29]. This value was used to evaluate the concentration of the penetrant in the polymer phase at sorption equilibrium. As evident from Fig. 10, these results are in good agreement with the results obtained from the barometric measurements and from FTIR Spectroscopy applied to the gas phase in tests α. Notably, this comparison also supports the assumption that the molar absorptivity of the absorbed CO_2 signal is temperature independent in the range investigated. The two spectroscopic approaches investigating the gas phase spectrum and the spectrum of the absorbed penetrant can be both easily extended to the case of sorption of gas mixtures, as discussed in the following section.

4.3. Sorption of gas mixtures in polymers: preliminary results

Sorption of multiple penetrants from a gas mixture can be investigated by means of FTIR Spectroscopy analyzing the spectra of the penetrant species both in the gas and the polymer phases with the same approach used for the investigation of sorption of pure substances. It is assumed that the molar absorptivity associated to the analytical peaks does not depend on the presence of other components. This hypothesis holds true for the system under investigation. We have preliminarly used the described experimental methodology to investigate sorption of CO_2–CH_4 gas mixture in PDMS. For the current configuration and for the intrinsic characteristic of the system at hand, the analysis could be performed only on the signals associated to carbon dioxide. To this aim, the IR gas calibration curves and the molar absorptivity of pure CO_2 absorbed in PDMS, as determined from the investigation of pure CO_2 reported above, were used. Gas mixtures of carbon dioxide and methane were prepared using mass flow controllers. Sorption tests α were conducted performing integral experiments up to 3.5 bar of total pressure. The IR gas concentration kinetics was studied following the procedure already explained in Section 4.2.2. Sorption tests β were conducted with integral steps up to a total pressure of approximately 5 bar and with dynamic experiments at greater pressures. A dynamic sorption test consists in introducing the gas mixture into the whole system so that the sorption and the filling processes occur simultaneously. The IR signal of absorbed CO_2 at 4954 cm^{-1} returns the concentration of the probe in the polymer at equilibrium for tests β, knowing that the molar absorptivity is equal to 0.2992 L cm^{-1} mol^{-1}. The partial pressure was evaluated from the IR gas phase signals at 4991 cm^{-1} as reported in Section 4.1. For tests α, the peak at 3626 cm^{-1} was chosen being one of the most sensitive and accurate IR signals at the thermodynamic conditions investigated.

During tests of α type, two factors prevented us from measuring sorption of CH_4 in PDMS from the CO_2/CH_4 gas mixture: the void volume and the sample mass. They are generally considered the most critical aspects of using barometry, i.e. the Pressure-Decay technique, but they can be tuned to improve the capability of the technique to measure the concentration of low sorbing gases in polymers. This is even more true when the IR absorbance decay approach is used because the sensitivity of the IR gas signals is lower than the pressure sensor one. We decided to use a unique specimen in order to allow a direct comparison of the barometric and IR sorption kinetics but multiple samples, even of different thickness, may be inserted in chamber 2. Tests of β type on the other hand did not allow us to identify the IR signal of methane absorbed in the polymer. From Eq. (1), being the molar absorptivity a constant, the specimen thickness could be tuned to increase the signal intensity at fixed thermodynamic conditions, i.e. at fixed molar concentration of gas in the polymer. Work is in progress to upgrade the instrumental apparatus for the concentration determination of low sorbing components and to resolve accurately the IR spectrum of methane absorbed in PDMS.

In Fig. 11 are compared the solubilities of carbon dioxide from gaseous mixtures of different composition (CO_2/CH_4 molar ratios respectively equal to 48/52 and 25/75) and from a pure gas phase. Data are reported in terms of concentration of CO_2 in PDMS as a function of partial pressure of CO_2 (in the case of mixtures) and of total pressure in the case of sorption of pure CO_2 gas. The analysis of the results puts in evidence how the solubility of carbon dioxide at a certain partial

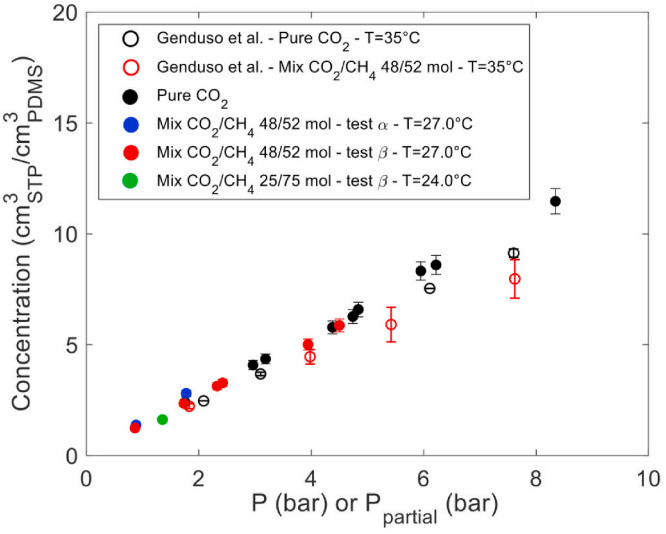

Fig. 11. Sorption of CO_2 in PDMS. Open symbols: data taken from the literature [11]. Full symbols: data produced in this work.

pressure, when in mixture with methane, is very close to the solubility of pure gaseous carbon dioxide at a pressure numerically equal to the partial pressure of CO_2 in the mixture, as also found by Genduso et al. [11]. Some deviation was observed from the data reported by Genduso et al. likely due to differences in the structure of the polymer and in the experimental techniques [11].

With respect to the classic approach based on gas chromatography, sorption thermodynamics and mass transport are investigated *in situ*. The IR gas phase approach may be applied to any gas mixture of *n* heteronuclear non-interacting chemical species. It may also be extended to systems of *n* low MW compounds one of which is homonuclear and, consequently, non-detectable with FTIR Spectroscopy. In this case, a thermodynamic model is required to identify its gas concentration. The specimen may be placed either in or out of the IR beam optical path, allowing the simultaneous investigation of sorption induced swelling. FTIR Spectroscopy is operated independently of barometry and allows the evaluation of sorption kinetics too. The spectroscopic uncertainty of the mole fraction composition is ± 0.001.

We would like to conclude this contribution with a few remarks on the differences with the ATR mode previously used by Hong, Barbari and Sloan to investigate diffusion of MEK/toluene vapor mixtures in polyisobutylene [18]. The authors performed sorption experiments with the same approach we have reported here as test of type β but without allowing the concentration of the two vapors to decrease during sorption. Specifically, they evaluated the composition of the binary vapor mixture at sorption equilibrium from a specific thermodynamic model for the activity of the two species. The method we propose complement their approach by allowing the determination of the gas or vapor composition from the IR measurement itself. Moreover, the ATR mode is usually applied with liquids or solid samples because adhesion with the crystal must be guaranteed during the measurement [15–20]. This is not a trivial aspect since gas concentration measurements are hindered and mass transport in polymers (for instance drying or sorption induced swelling) inevitably affects the contact with the ATR crystal. The latter aspect is even more important when quantifying sorption induced swelling: the sample is constrained to the crystal or directly cast on it [32]. Also, the penetrant concentration influences the refractive index of the medium and consequently the IR absorbance intensity [31]. The previous problems are absent when resorting to the transmission mode. FTIR Spectroscopy in the transmission mode is a versatile solution to study transport properties of low MW compounds – polymer systems.

5. Conclusions

FTIR Spectroscopy in transmission mode has been used to quantify sorption of pure carbon dioxide and methane in PDMS up to 9 bar at ambient temperature, adopting two approaches, one based on the analysis of the gas phase surrounding the polymer sample and the other based on the analysis of the condensed phase. To this aim, barometry has been first used to calibrate the FTIR signals in the gas phase. Then, pure gas sorption experiments were conducted. The decay of molar concentration in the gas phase was determined from the decrease of the IR absorbance of the species being absorbed by the polymer. The penetrant concentration within the polymer was then estimated from a molar balance. This method was also validated by comparison with simultaneous pressure-decay measurements. Sorption experiments were also performed collecting the IR spectrum of absorbed gas in the condensed phase, limiting the analysis to the case of CO_2, since no detectable signals were observed for CH_4. Notably, the two types of measurement produced coincident results.

These two straightforward IR approaches can be easily applied to investigate sorption of gas mixtures, a kind of measurement that is currently very difficult to perform. In this regard, we have presented here preliminary results for the sorption of carbon dioxide in PDMS from 48/52 and 25/75 by mol CO_2/CH_4 mixtures. The absorbed amount of methane from the same mixtures was not detectable due to limitations of the current experimental configuration (in terms of void volumes and sample mass). In the thermodynamic range investigated, it is worth noting that the absorbed amount of CO_2 at each partial pressure is very close to the values determined for the sorption of pure gas at pressure values corresponding to those of the CO_2 partial pressure in the mixture.

The benefits of using FTIR Spectroscopy to investigate sorption of pure and mixed gases in polymers are manifold. When dealing with the sorption of gas mixtures in polymers, FTIR Spectroscopy results to be more experimentally straightforward for estimating the concentration of each penetrant as compared to other techniques currently in use, such as Gas Chromatography. Moreover, *in situ* FTIR Spectroscopy allows a precise monitoring of sorption kinetics. Finally, the IR spectrum is rich of information and can be exploited to investigate host-guest molecular interaction, to quantify sample swelling and to study sorption-induced structural modifications (e.g. crystallization of amorphous regions or melting of crystalline domains).

CRediT author statement

V.L.: Conceptualization, Methodology, Validation, Investigation, Formal analysis, Writing – original draft, Writing – review and editing; G.S. and A.B.: Data curation, Software, Visualization; P.M.: Writing – review and editing, Resources, Supervision; G. M.: Writing – review and editing, Resources, Supervision, Project administration, Funding acquisition. All authors have given approval to the final version of the manuscript.

Fundings

This research did not receive any specific grant from funding agencies in the public, commercial, or not-for-profit sectors.

Declaration of competing interest

The authors declare that they have no known competing financial interests or personal relationships that could have appeared to influence the work reported in this paper.

Acknowledgement

The authors would like to thank Dr. Rezvan Jamaledin and Dr. Raffaele Vecchione of Center for Advanced Biomaterials for Health Care

(CABHC@CRIB) Italian Institute of Technology for providing the polydimethylsiloxane samples used in this work.

Appendix A. Supplementary data

Supplementary data to this article can be found online at https://doi.org/10.1016/j.memsci.2022.120445.

References

[1] D.S. Sholl, R.P. Lively, Seven chemical separations to change the world, Nature 532 (2016) 435–437, https://doi.org/10.1038/532435a.

[2] R.P. Lively, D.S. Sholl, From water to organics in membrane separations, Nat. Mater. 16 (2017) 276–279, https://doi.org/10.1038/nmat4860.

[3] M. Galizia, W.S. Chi, Z.P. Smith, T.C. Merkel, R.W. Baker, B.D. Freeman, 50th anniversary perspective: polymers and mixed matrix membranes for gas and vapor separation: a review and prospective opportunities, Macromolecules 50 (20) (2017) 7809–7843, https://doi.org/10.1021/acs.macromol.7b01718.

[4] A hydrogen strategy for a climate-neutral Europe, communication from the commission to the European parliament, the council, the European economic and social committee and the committee of the regions, 2 2020-07-08. https://op.europa.eu/it/publication-detail/-/publication/5602f358-c136-11ea-b3a4-01aa75ed71a1.

[5] G. Bernardo, T. Araújo, T.D.S. Lopes, J. Sousa, A. Mendes, Advances in membrane technologies for hydrogen purification 45 (12) (2020) 7313–7338, https://doi.org/10.1016/j.ijhydene.2019.06.162.

[6] https://ec.europa.eu/eurostat/. (Accessed 27 October 2021).

[7] V. Loianno, S. Luo, Q. Zhang, R. Guo, M. Galizia, Gas and water vapor sorption and diffusion in a triptycene-based polybenzoxazole: effect of temperature and pressure and predicting of mixed gas sorption, J. Membr. Sci. 574 (2019) 100–111, https://doi.org/10.1016/j.memsci.2018.12.054.

[8] P. Musto, V. Loianno, G. Scherillo, P. La Manna, M. Galizia, G. Guerra, G. Mensitieri, Benzene-induced crystallization of PPO: a combined thermodynamic and vibrational spectroscopy study, Ind. Eng. Chem. Res. 59 (12) (2020) 5402–5411, https://doi.org/10.1021/acs.iecr.9b04563.

[9] E. Robens, S.A.A. Jayaweera, S. Kiefer, Balances: Instruments, Manufacturers, History, Springer, 2014.

[10] E.S. Sanders, W.J. Koros, H.B. Hopfenberg, V.T. Stannett, Mixed gas sorption in glassy polymers: Equipment design considerations and preliminary results, J. Membr. Sci. 13 (2) (1983) 161–174, https://doi.org/10.1016/S0376-7388(00)80159-3.

[11] G. Genduso, E. Litwiller, X. Ma, S. Zampini, I. Pinnau, Mixed-gas sorption in polymers via a new barometric test system: sorption and diffusion of CO2-CH4 mixtures in polydimethylsiloxane (PDMS), J. Membr. Sci. 577 (2019) 195–204, https://doi.org/10.1016/j.memsci.2019.01.046.

[12] O. Vopička, M.G. De Angelis, N. Du, N. Li, M.D. Guiver, G.C. Sarti, Mixed gas sorption in glassy polymeric membranes: II. CO_2/CH_4 mixtures in a polymer of intrinsic microporosity (PIM-1), J. Membr. Sci. 459 (2014) 264–276, https://doi.org/10.1016/j.memsci.2014.02.003.

[13] E. Ricci, F.M. Benedetti, A. Noto, T.C. Merkel, J. Jin, M.G. De Angelis, Enabling experimental characterization and prediction of ternary mixed-gas sorption in polymers: C2H6/CO2/CH4 in PIM-1, Chem. Eng. J. 426 (2021) 130715, https://doi.org/10.1016/j.cej.2021.130715.

[14] S.C. Fraga, M. Monteleone, M. Lanč, E. Esposito, A. Fuoco, L. Giorno, K. Pilnáček, K. Friess, M. Carta, N.B. McKeown, P. Izák, Z. Petrusová, J.G. Crespo, C. Brazinha, J.C. Jansen, A novel time lag method for the analysis of mixed gas diffusion in polymeric membranes by on-line mass spectrometry: method development and validation, J. Membr. Sci. 561 (2018) 39–58, https://doi.org/10.1016/j.memsci.2018.04.029.

[15] V.V. Lavrent'ev, V.Y. Popov, R.M. Vasenin, Study of diffusion in boundary layers of polymer films by repeated disturbed full internal reflection of IR spectra, Polym. Sci. 17 (7) (1975) 1869–1872, https://doi.org/10.1016/0032-3950(75)90198-7.

[16] N.E. Schlotter, P.Y. Furlan, Small molecule diffusion in polyolefins monitored using the infrared, Vib. Spectrosc. 3 (1992) 147–153, https://doi.org/10.1016/0924-2031(92)80008-.

[17] S.U. Hong, T.A. Barbari, J.M. Sloan, Diffusion of methyl Ethyl Ketone in polyisobutylene: comparison of spectroscopic and gravimetric techniques, J. Pol. Sci. B: Polymer Physics 35 (8) (1997) 1261–1267, https://doi.org/10.1002/(SICI)1099-0488(199706)35:8%3C1261::AID-POLB12%3E3.0.CO, 2-6.

[18] S.U. Hong, T.A. Barbari, J.M. Sloan, Multicomponent diffusion of methyl Ethyl Ketone and toluene in polyisobutylene from vapor sorption FTIR-ATR spectroscopy, J. Pol. Sci. B: Polymer Physics 36 (2) (1998) 337–344, https://doi.org/10.1002/(SICI)1099-0488(19980130)36:2%3C337::AID-POLB12%3E3.0.CO;2-I.

[19] A.V. Ewing, S.G. Kazarian, Current trends and opportunities for the applications of in situ vibrational spectroscopy to investigate the supercritical fluid processing of polymers, J. Supercrit. Fluids 134 (2018) 88–95, https://doi.org/10.1016/j.supflu.2017.12.011.

[20] B.M. Carter, B.M. Dobyns, B.S. Beckingham, D.J. Miller, Multicomponent transport of alcohols in an anion exchange membrane measured by in-situ ATR FTIR spectroscopy, Polymer 123 (2017) 144–152, https://doi.org/10.1016/j.polymer.2017.06.070.

[21] G. Mensitieri, G. Scherillo, C. Panayiotou, P. Musto, Towards a predictive thermodynamic description of sorption processes in polymers: the synergy between theoretical EoS models and vibrational spectroscopy, Mater. Sci. Eng. R 140 (2020) 100525, https://doi.org/10.1016/j.mser.2019.100525.

[22] J. Kärger, T. Binder, C. Chmelik, F. Hibbe, H. Krautscheid, R. Krishna, J. Weitkamp, Microimaging of transient guest profiles to monitor mass transfer in nanoporous materials, Nat. Mater. 13 (2014) 333–343, https://doi.org/10.1038/nmat3917.

[23] S. Hwang, R. Semino, B. Seoane, M. Zahan, C. Chmelik, R. Valiullin, M. Bertmer, J. Haase, F. Kapteijn, J. Gascon, G. Maurin, J. Kärger, Revealing the transient concentration of CO2 in a mixed-matrix membrane by IR microimaging and molecular modeling, Angew. Chem. Int. Ed. 57 (2018) 5156–5160, https://doi.org/10.1002/anie.201713160.

[24] D. Carter, F.H. Tezel, B. Kruczek, J. Kärger, C. Chmelik, Determination of the adsorption isotherms and transport diffusivities of gases in mixtures inside zeolitic crystals using Infra-Red Micro-imaging, MethodsX 7 (2020) 100993, https://doi.org/10.1016/j.mex.2020.100993.

[25] S. Cotugno, D. Larobina, G. Mensitieri, P. Musto, G. Ragosta, A novel spectroscopic approach to investigate transport processes in polymers: the case of water–epoxy system, Polymer 42 (15) (2001) 6431–6438, https://doi.org/10.1016/S0032-3861(01)00096-9.

[26] M. Galizia, P. La Manna, M. Pannico, G. Mensitieri, P. Musto, Methanol diffusion in polyimides: a molecular description, Polymer 55 (4) (2014) 1028–1039, https://doi.org/10.1016/j.polymer.2014.01.009.

[27] A. Correa, A. De Nicola, G. Scherillo, V. Loianno, D. Mallamace, F. Mallamace, H. Ito, P. Musto, G. Mensitieri, A molecular interpretation of the dynamics of diffusive mass transport of water within a glassy polyetherimide, Int. J. Mol. Sci. 22 (2021) 2908, https://doi.org/10.3390/ijms22062908.

[28] V. Loianno, K.P. Bye, M. Galizia, P. Musto, Plasticization mechanism in polybenzimidazole membranes for organic solvent nanofiltration: molecular insights from in situ FTIR spectroscopy, J. Polym. Sci. 58 (2020) 2547–2560, https://doi.org/10.1002/pol.20200151.

[29] V. Loianno, A. Baldanza, G. Scherillo, R. Jamaledin, P. Musto, G. Mensitieri, A hyphenated approach combining pressure-decay and in-situ FT-NIR spectroscopy to monitor penetrant sorption and concurrent swelling in polymers, Ind. Eng. Chem. Res. 60 (2021) 5494–5503, https://doi.org/10.1021/acs.iecr.1c00264.

[30] National Institute of, Standard and technology (NIST9 reference fluid thermodynamic and transport properties database (REFPROP version 7), 10/09/21, https://webbook.nist.gov/chemistry/fluid/.

[31] N.M.B. Flichy, S.G. Kazarian, C.J. Lawrence, B.J. Briscoe, An ATR−IR study of poly(dimethylsiloxane) under high-pressure carbon dioxide: simultaneous measurement of sorption and swelling, J. Phys. Chem. B 106 (2002) 754–759, https://doi.org/10.1021/jp012597q.

[32] M. Giacinti Baschetti, E. Piccinini, T.A. Barbari, G.C. Sarti, Quantitative analysis of polymer dilation during sorption using FTIR-ATR spectroscopy, Macromolecules 36 (2003) 9574–9584, https://doi.org/10.1021/ma0302457.

[33] M.G. De Angelis, T.C. Merkel, V.I. Bondar, B.D. Freeman, F. Doghieri, G.C. Sarti, Hydrocarbon and fluorocarbon solubility and dilation in poly(dimethylsiloxane): comparison of experimental data with predictions of the Sanchez–Lacombe Equation of state, J. Pol. Sci.: Part B: Polymer Physics 37 (1999) 3011–3026, https://doi.org/10.1002/(SICI)1099-0488(19991101)37:21%3C3011::AID-POLB11%3E3.0.CO;2-V.

[34] T.C. Merkel, V.I. Bondar, K. Nagai, B.D. Freeman, I. Pinnau, Gas sorption, diffusion, and permeation in poly(dimethylsiloxane), J. Pol. Sci. B: Polymer Physics 38 (2000) 415–434, https://doi.org/10.1002/(SICI)1099-0488(20000201)38:3<415::AID-POLB8>3.0.CO;2-Z.

[35] V. M. Shah, B. J. Hardy, S.A. Stern, Solubility of carbon dioxide, methane, and propane in silicone polymers: effect of polymer side chains, J. Polym. Sci., Part B: Polym. Phys. (19869, 24, 2033−2047. https://doi.org/10.1002/polb.1986.090240910.

[36] D.S. Pope, W.J. Koros, G.K. Fleming, Measurement of thickness dilation in polymer films, J. Polym. Sci., Part B: Polym. Phys. 27 (1989) 1173–1177, https://doi.org/10.1002/polb.1989.090270516.

[37] M. Rezakazemi, K. Shahidi, T. Mohammadi, Sorption properties of hydrogen-selective PDMS/zeolite 4A mixed matrix membrane, Int. J. Hydrogen Energy 37 (22) (2012) 17275–17284, https://doi.org/10.1016/j.ijhydene.2012.08.109.